HHS Public Access

Author manuscript

Cell Metab. Author manuscript; available in PMC 2017 March 08.

Published in final edited form as:

Cell Metab. 2016 March 8; 23(3): 492–504. doi:10.1016/j.cmet.2016.01.001.

Intestinal phospholipid remodeling is required for dietary lipid uptake and survival on a high-fat diet

Bo Wang[1,2], **Xin Rong**[1,2], **Mark A. Duerr**[4], **Daniel J. Hermanson**[5], **Per Niklas Hedde**[6,7], **Jinny S. Wong**[8], **Thomas Q. de Aguiar Vallim**[3], **Benjamin F. Cravatt**[5], **Enrico Gratton**[6,7], **David A. Ford**[4], and **Peter Tontonoz**[1,2,9]

[1] Department of Pathology and Laboratory Medicine, University of California, Los Angeles, CA 90095, USA

[2] Howard Hughes Medical Institute, University of California, Los Angeles, CA 90095, USA

[3] Division of Cardiology, Department of Medicine, University of California, Los Angeles, CA 90095, USA

[4] Department of Biochemistry and Molecular Biology, and Center for Cardiovascular Research, Saint Louis University, St. Louis, MO 63104, USA

[5] The Skaggs Institute for Chemical Biology, Department of Chemical Physiology, The Scripps Research Institute, La Jolla, CA 92037 USA

[6] Laboratory of Fluorescence Dynamics, Biomedical Engineering Department, University of California, Irvine, Irvine, CA 92697, USA

[7] Center for Complex Biological Systems, University of California, Irvine, Irvine, CA 92697, USA

[8] Electron Microscopy Core, Gladstone Institute of Cardiovascular Disease, San Francisco CA 94158, USA.

Summary

Phospholipids are important determinants of membrane biophysical properties, but the impact of membrane acyl chain composition on dietary lipid absorption is unknown. Here we demonstrate that the LXR-responsive phospholipid-remodeling enzyme Lpcat3 modulates intestinal fatty acid and cholesterol absorption and is required for survival on a high-fat diet. Mice lacking Lpcat3 in the intestine thrive on carbohydrate-based chow, but lose body weight rapidly and become moribund on a triglyceride-rich diet. Lpcat3-dependent incorporation of polyunsaturated fatty

[9]Correspondance: Peter Tontonoz, MD PhD, David Geffen School of Medicine, University of California, Los Angeles, Los Angeles, CA 90095, USA, ptontonoz@mednet.ucla.edu.

Author Contributions

B.W., X.R., M.A.D, D.J.H., P.N.H., J.S.W., T.Q.V. performed experiments. B.W., X.R., D.J.H., P.N.H., J.S.W., B.F.C., E.G., D.A.F. and P.T. designed experiments. P.T., B.W. and D.A.F. wrote the paper.

Conflict of Interest Statement

None of the authors have a financial interest related to this work.

acids into phospholipids is required for the efficient transport of dietary lipids into enterocytes. Furthermore, loss of Lpcat3 amplifies the production of gut hormones including GLP-1 and oleoylethanolamide in response to high-fat feeding, contributing to the paradoxical cessation of food intake in the setting of starvation. These results reveal that membrane phospholipid composition is a gating factor in passive lipid absorption, and implicate LXR-Lpcat3 signaling in a gut-brain feedback loop that couples absorption to food intake.

Graphical Abstract

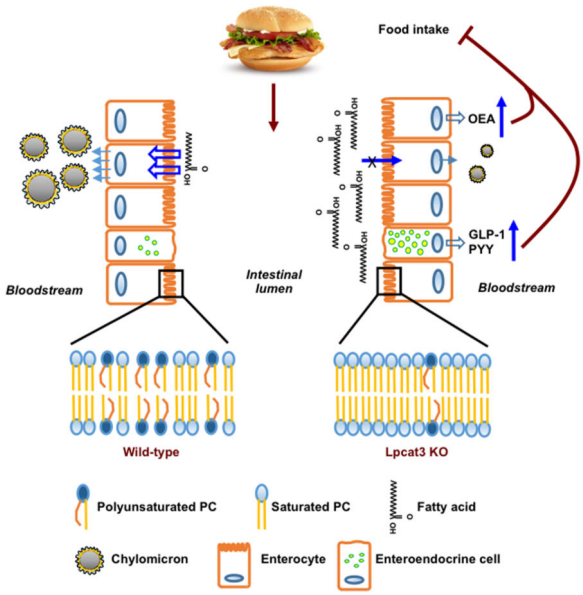

Introduction

Phospholipid composition is an important determinant of membrane biophysical properties. It is therefore reasonable to hypothesize that changes in the incorporation of polyunsaturated acyl chains into phospholipids might impact lipid transport across cellular membranes. However, it has heretofore been difficult to test this idea, as experimental systems that would allow selective alteration of phospholipid abundance in living animals have not been available. It has been speculated that reduced abundance of the essential fatty acid linoleate in intestinal membranes may be linked to malabsorption (Clark et al., 1973; Werner et al., 2002). Essential fatty acid (EFA) deficiency was reported to be associated with fat malabsorption in the 1940s (Richard H. Barnes et al., 1941), but the underlying mechanisms have remained obscure. Studies have suggested that defects in one or more intracellular events, including fatty acid uptake, triglyceride re-esterification, and chylomicron secretion, may contribute to reduced fat absorption in EFA deficiency (Clark et al., 1973; Levy et al., 1992; Werner et al., 2002). But how the loss of EFAs may affect these processes is unknown. To date, the hypothesis that altered membrane composition could affect lipid absorption *in vivo* has not been tested.

It has long been debated whether fatty acids are transported across the enterocyte apical membrane via passive diffusion or by carrier-mediated processes (Tso et al., 2004). Several

candidate fatty acid transporters have been characterized, including FATP4 and CD36 (Harmon et al., 1992; Stahl et al., 1999; Tso et al., 2004). Although conflicting results have been reported, deletion of either CD36 or FATP4 alone in mouse intestine does not appear to dramatically alter fatty acid uptake (Goudriaan et al., 2002; Nauli et al., 2006; Shim et al., 2009). Studies utilizing cultured cell systems have supported a passive diffusion model by showing that the rate of fatty acid uptake is linear, protease-resistant, and temperature-independent (Chow and Hollander, 1979; Ling et al., 1989; Trotter et al., 1996). By contrast, others have pointed to a carrier-mediated model based on observations that fatty acid uptake is saturable and competitive with other fatty acids (Ho and Storch, 2001; Murota and Storch, 2005). While the preponderance of *in vitro* data support a principal role for diffusion, testing the contribution of passive diffusion *in vivo* has been difficult due to the lack of an appropriate model system. No genetic mutation has been reported that directly affects passive fatty acid uptake in animals.

We recently identified a nuclear receptor pathway for dynamic modulation of membrane phospholipid composition in response to changes in cellular lipid metabolism (Rong et al., 2013). Ligand activation of liver X receptors (LXRs) preferentially drives the incorporation of polyunsaturated fatty acids into phospholipids through induction of the remodeling enzyme lysophosphatidylcholine acyltransferase 3 (Lpcat3). Loss of Lpcat3 in liver selectively reduces arachidonoyl phosphatidylcholine (PC) in liver membranes, leading to decreased membrane fluidity and curvature, and impaired VLDL secretion (Rong et al., 2015; Hashidate-Yoshida et al., 2015). The ability to regulate Lpcat3 activity has provided an unprecedented opportunity to test the physiologic consequences of changing membrane phospholipid composition *in vivo*.

Here we demonstrate that Lpcat3 deficiency in the intestine leads to a selective defect in the ability to incorporate the EFAs linoleate and arachidonate into phospholipids. We further show that this deficiency leads to marked changes in the biophysical properties of intestinal membranes and impairs passive fatty acid transport into enterocytes and chylomicron production. Lpcat3-deficiency in the setting of a triglyceride-rich diet leads to the exacerbated production of gut hormones and the cessation of food intake despite starvation. These data provide direct evidence for the critical importance of membrane phospholipid acyl chain composition in gating passive dietary lipid uptake and determining feedback responses to ingestion of a lipid-rich diet.

Results

Loss of Lpcat3 in intestine decreases plasma TG and cholesterol levels

We previously reported that mice deficient in Lpcat3 expression in the intestine (herein referred to as Lpcat3 IKO or IKO mice) showed severe post-natal growth retardation and failure to thrive (Rong et al., 2015). Surprisingly, however, we found that a minority of the pups could survive until weaning. Furthermore, once the surviving pups were weaned onto chow diet (13.5% calories from fat, 0.02% cholesterol) at 4 weeks of age, they grew rapidly and ultimately reached a similar size as their littermates (**Figure 1A**). Analysis of plasma lipid levels revealed lower serum TG and total cholesterol levels in Lpcat3 IKO mice compared to Lpcat3-floxed, Cre-negative controls (**Figure 1B**). There was no difference in

plasma non-esterified free fatty acid (NEFA) levels between groups. Blood glucose levels were slightly lower in the KO mice. Fractionation of plasma lipoproteins showed lower levels of TG in the VLDL fraction, and cholesterol in HDL fraction, in Lpcat3 IKO mice (**Figure 1C**).

Unexpectedly, and in contrast to our observations in suckling 1-week-old pups (Rong et al., 2015), we did not observe lipid accumulation in enterocytes of adult IKO mice (**Figure 1D**). Rather, we observed hypertrophy of mucosal villi in the duodenum and jejunum. Each villus contained multiple distorted branches, consistent with compensatory enlargement of the absorptive surface (Skala and Konradova, 1969). In line with the hypertrophy of villi, the small intestine was significantly longer in Lpcat3 IKOs than in controls (**Figure 1E**). We previously reported that Lpcat3 is an LXR target in liver and intestine (Rong et al., 2015). We found that intestinal Lpcat3 expression is also regulated by the fatty acid sensor peroxisome proliferator-activated receptor δ (PPARδ). Administration of GW742 (a potent PPARδ agonist) to mice increased Lpcat3 expression in the intestine (**Figure 1F**).

Lpcat3 is required for survival on a high-fat or western diet

Since Lpcat3 IKO pups showed severe growth retardation and lethality when suckling on lipid-rich milk (Rong et al., 2015), we tested how adult mice responded to diets rich in fat. We first fed mice a high-fat diet (60% calories from fat, 0.028% cholesterol) starting at 8- to 10-weeks of age–a time at which when floxed control and Lpcat3 IKO mice were of similar body weight. Surprisingly, Lpcat3 IKO mice lost ~20% of their body weight within 10 days and became moribund, necessitating termination of the study (**Figure 2A**). Similar rapid weight loss and failure to thrive was also observed in Lpcat3 IKO mice on a western diet (40% calories from fat, 0.2% cholesterol; **Figure 2B**). IKO mice lost ~20% of their body weight after 1 week of feeding, and one mouse died on day 4. Interestingly, the decline of Lpcat3 IKO mice on high-fat or western diet was reversible. Lpcat3 IKO mice fed high-fat diet recovered their body weight within two days when switched back to chow diet (**Figure 2C**). Furthermore, there was no difference in weight loss between HFD and western diet fed IKO mice (**Figure 2D**), indicating that the triglyceride rather than the cholesterol content of the western diet is the primary cause of weight loss. IKO mice actually gained slightly more weight when fed a high-cholesterol diet (13.5% calories from fat, 1.25% cholesterol) compared to controls (**Figure S1A**).

Magnetic Resonance Imaging (MRI) analysis of body composition showed that the weight loss after high fat or western diet feeding was primarily due to loss of body fat (**Figure 2E**). Remarkably, blood glucose levels in both high-fat and western diet-fed Lpcat3 IKO mice were markedly lower than those in control mice (**Figure 2F**). Intestinal morphology in high fat-fed IKO mice was similar to that of chow diet fed Lpcat3 IKO mice, with hypertrophy of villi and the absence of lipid accumulation in enterocytes (**Figure 2G**). Compared to control mice, there was no difference in the infiltration of inflammatory cells into the intestine of IKO mice fed a high-fat diet. Moreover, there was no difference in the expression of inflammatory cytokines or chemokine receptors between control and IKO intestine (**Figure 2H**). These findings suggest that the weight loss is not due to acute induction of intestinal inflammation in response to high-fat diet. Interestingly, the livers of Lpcat3 IKO mice

showed steatosis. Coupled with the finding of hypoglycemia, this observation suggested that the Lpcat3 IKO mice were starving. Gene expression analysis revealed significant reduction in the expression of *Ppara* and genes involved in fatty acid oxidation (**Figure S1B**), a finding consistent with reduced fatty acid availability in the liver.

Lpcat3 deficiency reduces food intake on high-fat diet through GLP-1 induction

Next we sought to understand the cause of the striking weight loss in IKO mice fed high-fat diet. We first monitored daily food consumption in individually-housed mice. Although Lpcat3 IKO mice consumed a similar amount of food as controls when fed chow diet (**Figure 3A**), they ate less than half as much as controls upon switching to 60% high-fat or western diet (**Figure 3B** and **S2A**). To determine if the reduced food intake was the sole cause of weight loss in Lpcat3-deficeint mice, we performed a pair-feeding study. As shown in Figure 3D, control mice limited to the same amount of high-fat diet consumed by the IKO mice lost ~7% of their body weight within one week, compared to ~17% for the Lpcat3 IKO mice. Body fat composition in Lpcat3 IKO after one week was 5%, compared to 10% in pair-fed controls (**Figure S2B**). These observations indicated that reduced food intake was a contributor, but not the only cause, of weight loss in IKO mice. Blood glucose levels were comparably reduced in Lpcat3 IKO and pair-fed controls (**Figure 3D**), suggesting that the hypoglycemia of IKO mice was largely due to starvation.

Next we investigated the etiology of reduced food consumption in Lpcat3-deficient mice. We fasted mice overnight, offered them both high-fat and chow diet, and monitored their food preference for 24 h. Interestingly, both control and IKO mice preferred the high-fat diet, and consumed the same amount of high-fat diet during the first 2 h (**Figure 3E**). After 2 h, control mice continued to eat almost exclusively high-fat diet and consumed only a minimal amount of chow. By contrast, the IKO mice stopped eating after the first 2 h and consumed neither diet. No difference in food intake was observed when the mice were refed with chow diet in a similar experiment (**Figure S2C**). Surprisingly, the IKO mice actually consumed slightly more food on high-cholesterol diet (**Figure S2D**). These observations suggested that dietary fat was inhibiting total food intake in Lpcat3 IKO mice, regardless of the type of food offered.

Previous studies have identified gut-derived hormones that are induced by dietary fat, including GLP-1, PYY and CCK (Begg and Woods, 2013; Camilleri, 2015). To determine whether any of these mediators were in play in Lpcat3-deficient mice, we measured their levels in the plasma of high-fat fed mice. Remarkably, active GLP-1 levels were 6-fold higher, and PYY levels were 3-fold higher in Lpcat3 IKO mice compared to controls (**Figure 3F**). There was no difference in CCK levels. Interestingly, GLP-1 levels were also increased by 3-fold in chow diet-refed IKO mice, while PYY levels were not changed (**Figure S2E**). To test whether this induction of GLP-1 was contributing to the reduction in food intake, we injected mice with the GLP-1 receptor antagonist exendin-(9-39) (Ex-9) and monitored food intake during fasting/refeeding. Compared to vehicle treatment, Ex-9 treatment increased high-fat diet consumption in IKO mice to similar levels as control mice during the first 6 h (**Figure S2F**). Similarly, chronic Ex-9 treatment over the course of 4 days partially rescued food intake and weight loss in high-fat diet-fed IKO mice (**Figure 3G**

and S2G). These findings indicate that excessive GLP-1 signaling contributes to the food intake phenotype of Lpcat3-deficient mice.

The partial rescue of food intake by GLP-1 receptor antagonist indicates that additional anorexic pathways are also involved. N-acylphosphatidylethanolamine (NAPE) and oleoylethanolamide (OEA) are induced by fat digestion and inhibit food intake through interactions with the central nervous system (Gillum et al., 2008) (Fu et al., 2003; Schwartz et al., 2008). The endocannabinoids, anandamide (AEA) and 2-arachidonoyl glycerol (2-AG) increase food intake in fasted mice via activation of cannabinoid type-1 (CB1) receptors (Soria-Gomez et al., 2014). Quantitation by mass spectrometry revealed that OEA levels were significantly increased in the serum and jejunum of high-fat diet refed IKO mice compared to controls (**Figure 3H**), whereas total NAPE levels were not significantly altered in the intestine and slightly decreased in the serum (**Figure S3A**). High-fat diet refeeding had no effect on the levels of AEA in the intestine of IKO mice (**Figure S3A**). Levels of 2-AG were not consistently altered in the serum or intestine of IKO mice (**Figure S3A and S3B**). These data suggest that OEA may also contribute to the reduced high-fat diet consumption in IKO mice.

Loss of intestinal Lpcat3 protects from diet-induced obesity

Since Lpcat3 IKO mice thrive on chow (13.5% fat), but cannot tolerate the standard 60% or 40% fat content diets commonly used to induce obesity in mice, we tested their ability to survive on a moderate-fat diet (30% calories from fat, 0.02% cholesterol). Although IKO mice initially consumed less food than controls when switched to this diet, they appeared to adapt, as their food intake was comparable to controls after several weeks of feeding (**Figure 4A**). Despite similar food consumption, however, Lpcat3 IKO mice gained much less body weight after 17 weeks of feeding (**Figure 4B**). Diet-induced obesity is frequently accompanied by glucose intolerance. There was no difference in glucose tolerance between control and Lpcat3 IKO mice maintained on chow diet (**Figure 4C**), but Lpcat3 IKO mice showed improved glucose tolerance compared to controls when maintained on moderate-fat (30%) diet (**Figure 4D**).

To investigate potential mechanisms underlying the protection from diet-induced obesity in Lpcat3 IKO mice, we assessed lipid absorption by measuring fecal lipid content. IKO mice produced 35% more feces per gram of food intake than controls (**Figure 4E**). Furthermore, fecal NEFA and cholesterol levels were 4- to 5-fold higher in IKO mice (**Figure 4F**). Absorption coefficients for NEFA and cholesterol in Lpcat3 IKO mice were reduced compared to control mice, suggesting malabsorption of NEFA and cholesterol. By contrast, fecal TG levels were negligible in both groups, and no difference in the TG absorption coefficient was observed, indicating that loss of Lpcat3 does not impair hydrolysis of ingested TG. Consistent with this observation, there was no difference in biliary bile acid levels or bile acid composition between control and IKO mice (**Figure 4G** and **H**). Fecal lipid content was also higher in the IKO mice fed western diet (**Figure S4**).

Lpcat3 deficiency in intestine impairs fat absorption and chylomicron secretion

To directly test if Lpcat3 activity was required for transport of dietary fat absorption into the circulation, we performed postprandial TG response assays. Serum TG levels were dramatically reduced in IKO mice following an intragastric olive oil load (**Figure 5A**). We also measured plasma lipid levels in mice fasted overnight and then refed with 60% high-fat diet for 2 h. This challenge revealed 70% and 25% decreases in serum TG and cholesterol, respectively, in IKO compared to control mice (**Figure 5B**). In contrast, serum NEFA levels were 2-fold higher in IKO mice. Histological analysis of refed intestines showed an almost complete absence of lipid accumulation in enterocytes of Lpcat3 IKO duodenum and jejunum, whereas controls contained many lipid droplets (**Figure 5C)**. A similar phenomenon was observed in intestines of IKO mice gavaged with olive oil (**Figure S5**). These findings suggested that fatty acid (FA) uptake, TG synthesis and/or chylomicron secretion, was markedly reduced in Lpcat3-deficient enterocytes.

To directly visualize FA uptake into enterocytes, we gavaged mice with BODIPY-labeled FA together with olive oil, and examined enterocytes by microscopy. Abundant fluorescently-labeled lipid droplets were observed in control intestines, while almost no fluorescence was present in IKOs (**Figure 5D**), indicative of a major defect in FA absorption. We also assessed FA uptake in mice deficient in Cd36 (Chen et al., 2001; Nassir et al., 2007). Although there was a subtle decrease in fluorescence signal in Cd36 KO enterocytes compared to wild-type controls, loss of Lpcat3 had a much more severe impact (**Figure 5D**). Furthermore, analysis of intestinal uptake of radiolabeled fatty acid in response to oral dosing of ^{14}C-trioleoylglycerol revealed markedly reduced absorption in the proximal intestine of IKO mice, and a compensatory shift in uptake to more distal segments (**Figure 5E**). To determine if absorption defect in IKO mice was specific for fatty acids, we assessed *in vivo* cholesterol uptake and *ex vivo* glucose uptake. There was no difference in labeled glucose uptake between control and IKO intestines (**Figure 5F**). Cholesterol absorption measured by the fecal dual isotope ratio method revealed a trend towards decreased uptake in IKO mice (**Figure 5G**). These observations indicate that not all metabolite transport pathways are compromised in the IKO mice and that the uptake of fatty acids, and to a lesser degree cholesterol, into enterocytes is preferentially affected.

We next investigated if intestinal Lpcat3 deficiency affects chylomicron assembly and secretion. Negative staining of plasma chylomicron fractions by EM revealed markedly smaller chylomicron particles in Lpcat3 IKO mice compared to controls (**Figure 6A** and **6B**), suggesting poor apoB lipidation. Consistent with reduced plasma TG levels and smaller chylomicron particle size, the plasma collected from Lpcat3 deficiency mice was transparent, while control plasma was milky after high-fat diet refeeding (**Figure 6C**). ApoB in the chylomicron fraction was decreased in Lpcat3 IKO mice, whereas total serum apoB was similar (**Figure 6D**). Together with increased apoB-48 in the duodenum of IKO mice (**Figure 6D**), these data indicate that chylomicron secretion is impaired in the setting of Lpcat3 deficiency (**Figure 6D**). Similar results were obtained in high-fat diet-fed mice (**Figure S6**). These findings are consistent with the reduced serum levels of triglyceride and cholesterol in IKO mice (Figure 1).

Regulation of intestinal membrane fluidity gates fatty acid uptake

To begin to explore mechanisms underlying defective lipid uptake and chylomicron production, we analyzed the expression of genes involved in FA uptake, TG synthesis, lipoprotein production, and intracellular FA transport. mRNA levels of most genes implicated in these processes were not reduced, and levels of some were actually increased in Lpcat3 IKO mice compared to controls in both the fasting and refed states (**Figures 6E** and **6F**). Thus, defects in lipid metabolic gene expression could not explain the phenotypes of IKO mice.

To gain insight into how the enzymatic activity of Lpcat3 was linked to these phenotypes, we performed lipidomic analyses. Previous studies have shown that Lpcat3 is uniquely required for the incorporation of arachidonate into phospholipids in liver, but that its loss does not affect the total abundance of PC (Rong et al., 2015). There was no difference in total levels of PC in enterocytes isolated from Lpcat3 IKO and control mice (**Figure S7A**). However, mass spectrometry analysis of individual PC species in chow diet-fed enterocytes revealed a selective decrease in 34:2 PC (predominantly species containing 16:0 and 18:2 acyl chains) abundance (**Figure 7A**). There was also a compensatory increase in the abundance of several PC species containing monounsaturated 18:1 chains. In contrast to prior results with the liver-specific Lpcat3 knockouts (Rong et al., 2015), there was only a small decrease in 38:4 PC (predominantly species containing 18:0 and 20:4 chains) abundance, perhaps reflecting the low abundance of arachidonoyl PC in enterocytes. Feeding the IKO and control mice a 60% high-fat diet for 5 days uncovered more dramatic differences in the abundance linoleoyl and arachidonoyl PC species (**Figure S7B**). Total PC levels were again not different between groups (**Figure S7C**).

Next we tested whether loss of Lpcat3 would alter the phospholipid composition of chylomicrons secreted from the intestine. Indeed, analysis of PC species in pooled chylomicron fractions isolated from mice gavaged with an olive oil bolus revealed a selective reduction in 34:2 PC (predominantly species containing 16:0 and 18:2 acyl chains) abundance in IKO chylomicrons (**Figure S7D**). Interestingly, the abundance of individual PC species in the livers of high-fat diet-fed IKO mice also resembled their abundance in the enterocytes, even though Lpcat3 activity was intact in these livers (**Figure S7E** and **S7F**). These findings suggest that the PC composition of the liver is at least in part dependent on intestinal Lpcat3 activity.

To further address whether changes in enterocyte fatty acid content or phospholipids composition were linked to the weight loss phenotype, we administered soy PC (63% 18:2-containing PC) or hydro soy PC (88.6% 18:0-containing PC) to IKO mice by oral gavage and monitored food intake and body weight. These diets would be expected to deliver increased levels of either 18:2 or 18:0 fatty acids to the intestinal epithelium, as PC is hydrolyzed by pancreatic phospholipase A2 to liberate fatty acids and lysoPC. However, once liberated, the 18:2 would be unable to be re-incorporated into PC in mice lacking Lpcat3. Neither diet was able to rescue body weight or food intake in the IKO mice (**Figure S7G** and **S7H**), consistent with the hypothesis that the change in phospholipids, rather than loss of polyunsaturated fatty acids, is the cause of the phenotype.

To understand how changes in enterocyte membrane phospholipid composition might lead to reduced lipid uptake, we performed biophysical studies of lipid movement in intestinal tissue *ex vivo* using live-cell imaging and laurdan staining. Laurdan is a fluorescent lipophilic molecule that can incorporate into membranes, sense the polarity of the membrane environment, and thus detect changes in membrane dynamics (Golfetto et al., 2013; Parasassi and Gratton, 1995). Changes in membrane dynamics shift the laurdan emission spectrum, which can be quantified by the generalized polarization (GP). The striking increase in GP (yellow/orange pseudocolor) in enterocytes lacking Lpcat3 is indicative of membranes with strongly reduced lipid mobility (**Figure 7B**). Thus, membranes are less dynamic, and their component lipids move less readily, in the absence of Lpcat3. In contrast, we did not find obvious differences in the ultrastructure of intestinal microvilli between control and IKO enterocytes by electron microscopy, suggesting that these changes in membrane composition do not grossly deform membrane structure (**Figure 7C**).

Evidence from isolated cells suggests that a passive transport dominates when the luminal FA concentration is high, but direct tests of this idea in living intestines is lacking. Thus, we reasoned that decreased membrane dynamics due to altered composition in the absence of Lpcat3 might be associated with impaired FA uptake into enterocytes. Supporting this notion, *ex vivo* fluorescent-FA uptake into enterocytes was 50% lower in IKO intestines compared to controls (**Figure 7D**). Moreover, administration of 16:0, 20:4 PC to IKO intestines 30 min prior to label administration increased FA uptake to a level comparable to control intestines (**Figure 7E**). The time frame of this rescue experiment strongly suggests that changes in enterocyte gene and protein expression are not required. In contrast, PC treatment had no effect on glucose uptake (**Figure 7F**). To further support our hypothesis that Lpcat3 was affecting passive transport, we performed additional *ex vivo* FA uptake assays at 4°C on ice, a condition under which active transport is inhibited. Compared to floxed intestines, IKO intestines showed a similar reduction in FA uptake at 4°C on ice as that observed at room temperature (**Figure 7G**). Furthermore, the administration of 16:0, 20:4 PC, but not 16:0,18:0 PC also increased FA uptake at 4°C (**Figure 7H**), indicating that polyunsaturated PC promotes passive FA uptake into cells.

Collectively, these results demonstrate that loss of Lpcat3 activity in the intestine leads to a selective defect in the ability to incorporate linoleate and arachidonate into phospholipids. This defects leads to marked biophysical changes in the membrane and is associated with impaired passive fatty acid transport into enterocytes.

Discussion

Dietary lipid absorption is a complex process involves several steps: intraluminal hydrolysis of dTG, FA and monoacylglycerol uptake, re-synthesis of TG, and chylomicron assembly and secretion (Abumrad and Davidson, 2012). Defects in several steps have been shown to affect fat absorption. Poor solubilization of dietary fat in bile-diverted animals greatly reduces fat absorption (Clark and Holt, 1968; Tso et al., 1978). Deficiency of acyl CoA:monoacylglycerol acyltransferase-2, an enzyme involved in TG re-synthesis, delays fat absorption (Yen et al., 2009). Loss of microsomal TG transfer protein (Mttp), which is required for chylomicron assembly, also leads to malabsorption (Xie et al., 2006). In

addition, PC has long been recognized to facilitate dietary lipid uptake, and studies in rats with bile fistulas showed that infusion of PC restored the lymphatic output of TG (Tso et al., 1977; Tso et al., 1981). However, beyond the obvious role of biliary PC in fat solubilization, it is unknown whether specific PC species also impact other steps of fat absorption. We have shown here that loss of Lpcat3 in intestine reduces the abundance of PC containing linoleate and arachidonate, and causes severe fat malabsorption. These findings implicate intestinal PC composition as a major determinant of dietary lipid uptake.

Our biophysical studies revealed that a reduction in linoleoyl and arachidonoyl PC in Lpcat3 IKO intestinal membranes, possibly together with an increase in saturated or monosaturated PC, results in a striking decrease in membrane fluidity. Membrane dynamics influence a variety of cellular processes, including transmembrane transport and intracellular vesicle trafficking (Spector and Yorek, 1985). Several steps during fat absorption could potentially be affected by changes in membrane dynamics, including fatty acid transport across the apical membrane of enterocytes, chylomicron transport from ER to Golgi, and secretion into lymphatic circulation. We find that these steps are indeed profoundly altered in Lpcat3-deficient intestine. We observed a reduction in fatty acid and cholesterol uptake, along with reduced chylomicron secretion, manifested by decreased chylomicron apoB and increased intestinal apoB levels. It seems likely that changes in membrane fluidity and dynamics in IKO enterocytes contribute to these defects, but further studies will be needed to establish a causal relationship.

Previously, we reported that Lpcat3 deficiency in liver leads to reduced arachidonoyl PLs and impaired transfer of TG to VLDL (Rong et al., 2015). Hashidate-Yoshida et al. observed an intestinal TG transport defect in newborn Lpcat3 global KO pups (Hashidate-Yoshida et al., 2015), which they attributed to severe enterocyte damage, including the loss of microvilli. They proposed that loss of PUFA in PLs changes membrane curvature, impairs TG transport to lipoproteins, and leads to lipid droplet accumulation and cellular damage. One caveat of global Lpcat3 KO studies, however, is that the mice are moribund and die within days after birth with multiple systemic defects (Rong et al., 2015; Hashidate-Yoshida et al., 2015). By contrast, the ultrastructure of enterocytes in adult Lpcat3 IKO mice is preserved and TG does not accumulate in enterocytes. Our data suggest that malabsorption in IKO mice is mainly due to defective fatty acid uptake and impaired intracellular chylomicron metabolism.

Although putative transporters such as Cd36 and Fatp4 have been reported to be dispensable for FA uptake into enterocytes (Goudriaan et al., 2002; Nassir et al., 2007), the importance of passive transport under physiological conditions has been difficult to test directly due to the inability to manipulate membrane composition in living animals. Here we demonstrate that altering the enterocyte membrane itself affects FA uptake *in vivo*. Our data suggest that the increased membrane acyl chain saturation in IKO mice, and the consequent altered membrane dynamics, impede dietary FA uptake. Acute administration of polyunsaturated PC increased passive fatty acid uptake in Lpcat3-deficient intestine without affecting the active transport of glucose, indicating that altered membrane composition per se is the proximal cause of the defect. Our data are most consistent with the hypothesis that the increased abundance of polyunsaturated PC in the apical membrane facilitates the flip-flop

of fatty acids into the bilayer. Prior in vitro studies have shown that fatty acids move across membranes spontaneously and rapidly (Brunaldi et al., 2010; Kamp and Hamilton, 1992). Whether or not membrane composition also affects the downstream incorporation of fatty acids into triglycerides remains to be determined, but the formation of triglyceride droplets from dietary FA was also severely impaired in the Lpcat3 IKO mice. Our results provide *in vivo* support for the hypothesis that passive transport of fatty acids across a permissive enterocyte membrane predominates in the context of bolus lipid challenge *in vivo*.

Interestingly, the phospholipid profile of Lpcat3 KO enterocytes (decreased 18:2-containing PC, decreased 20:4-containing PC, and increased in 38:4 PC), is similar to that previously observed in EFA-deficient mucosa (Christon et al., 1989; Enser and Bartley, 1962; Yurkowski and Walker, 1971). EFA deficiency has been recognized to be associated with fat malabsorption for decades (Clark et al., 1973; Hjelte et al., 1990; Levy et al., 1992; Richard H. Barnes et al., 1941), but the underlying mechanisms have never been defined. It had been suggested that changes in phospholipid profiles in EFA-deficient intestine may be linked to malabsorption, but there has been no *in vivo* system available to test this idea. Our study provides a plausible explanation for why EFA are important for fat absorption. It is important to note that Lpcat3 IKO mice are not globally EFA-deficient; they only lack certain EFA in phospholipids. Our data suggest that loss of EFA-containing PC could be one possible contributor to malabsorption in EFA-deficiency, especially given that most alternative explanations have been ruled out (Werner et al., 2002).

Another unexpected finding of this study was the requirement for Lpcat3 activity for mice to survive on lipid rich diets. This unique phenotype appears to result from the combination of ineffective lipid absorption and dramatically reduced food intake. Once switched to a high-fat or western diet, Lpcat3 IKO mice stop eating. They continue to resist eating and rapidly lose body weight, even though they exhibit signs of starvation. Interestingly, the suppression of food intake is dependent on the amount of fat present in the diet. There was no difference in food consumption between IKO mice and controls on chow diet and they were able to adapt to tolerate a 30% fat diet after several days. These observations suggest that the inability to process dietary fat triggers one or more signals that inhibit food intake in Lpcat3 IKO mice. The fact that the mice are able to tolerate moderate-fat diet despite their severe FA uptake defect underscores the enormous absorptive capacity of the intestinal tract. The hyperplasia of the intestinal mucosa in IKO mice also probably helps to partially compensate for the defect.

GLP-1 and PYY were highly induced upon high-fat diet feeding in Lpcat3 IKO mice. These hormones are secreted from enteroendocrine L-cells in the distal small intestine, most likely in response to luminal FA. It is likely that reduced fat absorption in the duodenum and jejunum of IKO mice results in more FA reaching the ileum, where they trigger the secretion of gut hormones. Our data suggest that the excessive GLP-1 secretion contributes to anorexia in Lpcat3 KO mice, as a GLP-1 receptor antagonist partially rescued food intake. However, additional pathways must also be at play. High-fat feeding induces the biosynthesis of intestinal NAPE and OEA, which inhibit food intake by activating nuclei in the hypothalamus and peripheral sensory fibers (Provensi et al., 2014; Rodriguez de Fonseca et al., 2001). In this study, intestinal and serum OEA levels were hyper-induced in high-fat

diet refed IKO mice, suggesting a contribution to the reduced food consumption. However, given the severity of the anorexic response, we speculate that additional as yet unidentified mediators must also be involved.

In conclusion, these results highlight the critical importance of membrane phospholipid composition and dynamics in determining dietary lipid diffusion across the intestinal membrane and thereby controlling food consumption during high-fat feeding. Future studies will explore whether manipulating intestinal membrane phospholipid composition could be used as a strategy to modulate hyperlipidemia and diet-induced obesity.

Materials and Methods

Animal studies

Lpcat3$^{fl/fl}$ and *Lpcat3*$^{fl/fl}$; *Villin-Cre* mice have been described (Rong et al., 2015). *Cd36−/−* mice were obtained from Jackson Laboratory. All mice were housed under pathogen-free conditions in a temperature-controlled room with a 12-hr light/dark cycle. Mice were fed chow diet (LabDiet #5001), 60% fat diet (Research Diets # D12492), 30% fat diet (Research Diets # D11072204), western diet (Research Diets #D12079) or 1.25% cholesterol diet (Research Diets #C12826). All experiments were performed with male mice. Small intestines were excised and cut into three segments with length ratios of 1:3:2 (corresponding to duodenum, jejunum and ileum). Intestine tissues were frozen in liquid nitrogen and stored at −80°C or fixed in 10% formalin. Blood was collected by retro-orbital bleeding, and the plasma was separated by centrifugation. Plasma lipids were measured with the Wako L-Type TG M kit, the Wako Cholesterol E kit; and the Wako HR series NEFA-HR(2) kit. Tissue and fecal lipids were extracted with Folch lipid extraction (Folch et al., 1957) and measured with the same enzymatic kits. Plasma fast protein liquid chromatography (FPLC) lipoprotein profiles were performed in the Lipoprotein Analysis Laboratory at Wake Forest University. Animal experiments were conducted in accordance with the UCLA Animal Research Committee.

Lipid uptake

We assessed intestinal uptake of dietary fat as described (Yen et al., 2009). Mice were fasted for 4 h and gavaged with 1 μCi of 14C-trioleoylglycerol in 200 μl of olive oil. Two hours later, we excised the small intestine (between the base of the stomach and the cecal junction), flushed it with 0.5 mM sodium taurocholate in PBS and cut it into 2-cm segments. Segments were with 500 μl of 1 N NaOH at 65 °C overnight, mixed with ScintiSafe (Fisher Scientific) and scintillation counted. *In vivo* cholesterol absorption was determined by fecal dual isotope ratio as described (Temel et al., 2005). Absorption of dietary lipids was determined by subtracting the amount of each lipids excreted in feces in 72 h, from the amount of lipid ingested (net fat absorption). This quantity was subsequently expressed as a percentage of the amount of total lipids ingested in 72 h (coefficient of lipid absorption).

Imaging studies

Mice were fasted for 4 h and gavaged with BODIPY® 500/510 C1, C12 fatty acids (2 μg/g body weight, Molecular Probes #D3823) and olive oil (10 μl/g body weight) for 2h. Small

intestines were excised and frozen in OCT. 10 μm sections were cut, mounted with ProLong® Diamond Antifade Mountant with DAPI, and examined under fluorescence microscope. For determination of chylomicron size by transmission electron microscopy, mice were fasted overnight and refed 60% high fat diet for 2 h. 200 μl pooled plasma from 5 *Lpcat3*$^{fl/fl}$ and *Lpcat3*$^{fl/fl}$; *Villin-Cre* mice were overlaid with 600 μl saline and centrifuged at 50000 rpm for 5 h in a TLA 120.2 rotor and the chylomicron layer removed. For electron microscopy, 5 μl of the chylomicron fraction was applied to carbon-coated copper grids and stained with 2.0% uranyl acetate for 15 min. Grids were visualized with a JEOL 100CX transmission electron microscope. Particle diameter was measured using ImageJ.

Membrane dynamics

Membrane dynamics was analyzed as described with modifications (Golfetto et al., 2013). Briefly, duodenum from Lpcat3$^{fl/fl}$ and Lpcat3$^{fl/fl}$; Villin-Cre mice was excised, cut open and incubated with 0.15 mM Laurdan (6-dodecanoyl-2-dimethylaminonaphthalene; Invitrogen) at 37°C for 30 min. Tissues were rinsed with phosphate-buffered saline (PBS). Spectral data were acquired with a Zeiss LSM710 META laser scanning microscope coupled to a 2-photon Ti:Sapphire laser (Mai Tai, Spectra Physics, Newport Beach, CA) producing 80-fs pulses at a repetition of 80 MHz with two different filters: 460/80 nm and 540/50 nm. Spectral data were processed by the SimFCS software (Laboratory for Fluorescence Dynamics). The GP value was calculated for each pixel using the two Laurdan intensity images (460/80 nm and 540/50 nm). The GP value of each pixel was used to generate the pseudocolored GP image.

Ex vivo fatty acid uptake assay

Mice were fasted for 4 h and euthanized with isoflurane. The small intestine was rinsed in situ with PBS. The ends of duodenum segment (~5 cm) were clamped with hemostats forceps to make an intestine sac. The sac was filled with QBT fatty acid uptake assay solution mixed with 10 mM sodium taurocholate and 4 mM oleic acid. The sac was incubated with uptake assay solution for 1 and 2 min either at room temperature or at 4°C on ice. After incubation, the sac was removed and immediately immersed in ice-cold 0.5 mM sodium taurocholate in PBS to stop the reaction. The sac was washed twice with 0.5 mM sodium taurocholate in PBS, and scraped with a glass slide to obtain villi, which were further washed twice with 0.5 mM sodium taurocholate and homogenized with RIPA buffer. Fluorescence signal in the supernatant was read using a fluorescence plate reader with an excitation wavelength of 485 nm and an emission wavelength of 515 nm. Fluorescence was normalized to protein concentration. For PC treatment, intestinal sacs were filled with 25 μM 16:0; 18:0 control or 16:0; 20:4 PC liposome and incubated in PBS for 30 min. After incubation, intestines were washed with PBS followed prior to assessment of fatty acid uptake.

Statistical analysis

For all studies, results from quantitative experiments were expressed as means ± SEM. Where appropriate, significance was be calculated by Student's t test, one- or two-way ANOVA using Bonferroni multiple comparison.

Supplementary Material

Refer to Web version on PubMed Central for supplementary material.

Acknowledgements

We thank Jinkuk Choi, Ito Ayaka and Diana Shih for technical support. We thank Stephen Young, Karen Reue, and Peter Edwards for helpful discussions. This work was supported by grants HL090553, DK063491, HL030568, HL074214, GM103540, GM076516 and AHA Fellowship 13PRE17150049. P.T. is an Investigator of the Howard Hughes Medical Institute.

References

Abumrad NA, Davidson NO. Role of the gut in lipid homeostasis. Physiol Rev. 2012; 92:1061–1085. [PubMed: 22811425]

Begg DP, Woods SC. The endocrinology of food intake. Nat Rev Endocrinol. 2013; 9:584–597. [PubMed: 23877425]

Brunaldi K, Huang N, Hamilton JA. Fatty acids are rapidly delivered to and extracted from membranes by methyl-beta-cyclodextrin. J Lipid Res. 2010; 51:120–131. [PubMed: 19625735]

Camilleri M. Peripheral mechanisms in appetite regulation. Gastroenterology. 2015; 148:1219–1233. [PubMed: 25241326]

Chen M, Yang Y, Braunstein E, Georgeson KE, Harmon CM. Gut expression and regulation of FAT/CD36: possible role in fatty acid transport in rat enterocytes. Am J Physiol Endocrinol Metab. 2001; 281:E916–923. [PubMed: 11595646]

Chow SL, Hollander D. Linoleic acid absorption in the unanesthetized rat: mechanism of transport and influence of luminal factors on absorption. Lipids. 1979; 14:378–385. [PubMed: 35725]

Christon R, Even V, Daveloose D, Leger CL, Viret J. Modification of fluidity and lipid-protein relationships in pig intestinal brush-border membrane by dietary essential fatty acid deficiency. Biochim Biophys Acta. 1989; 980:77–84. [PubMed: 2538158]

Clark SB, Ekkers TE, Singh A, Balint JA, Holt PR, Rodgers JB Jr. Fat absorption in essential fatty acid deficiency: a model experimental approach to studies of the mechanism of fat malabsorption of unknown etiology. J Lipid Res. 1973; 14:581–588. [PubMed: 4729974]

Clark SB, Holt PR. Rate-limiting steps in steady-state intestinal absorption of trioctanoin-1-14C. Effect of biliary and pancreatic flow diversion. J Clin Invest. 1968; 47:612–623. [PubMed: 5637147]

Drover VA, Nguyen DV, Bastie CC, Darlington YF, Abumrad NA, Pessin JE, London E, Sahoo D, Phillips MC. CD36 mediates both cellular uptake of very long chain fatty acids and their intestinal absorption in mice. J Biol Chem. 2008; 283:13108–13115. [PubMed: 18332148]

Enser M, Bartley W. The effect of ;essential fatty acid' deficiency on the fatty acid composition of the total lipid of the intestine. Biochem J. 1962; 85:607–614. [PubMed: 16748978]

Folch J, Lees M, Sloane Stanley GH. A simple method for the isolation and purification of total lipides from animal tissues. J Biol Chem. 1957; 226:497–509. [PubMed: 13428781]

Fu J, Gaetani S, Oveisi F, Lo Verme J, Serrano A, Rodriguez De Fonseca F, Rosengarth A, Luecke H, Di Giacomo B, Tarzia G, et al. Oleylethanolamide regulates feeding and body weight through activation of the nuclear receptor PPAR-alpha. Nature. 2003; 425:90–93. [PubMed: 12955147]

Gillum MP, Zhang D, Zhang XM, Erion DM, Jamison RA, Choi C, Dong J, Shanabrough M, Duenas HR, Frederick DW, et al. N-acylphosphatidylethanolamine, a gut-derived circulating factor induced by fat ingestion, inhibits food intake. Cell. 2008; 135:813–824. [PubMed: 19041747]

Golfetto O, Hinde E, Gratton E. Laurdan fluorescence lifetime discriminates cholesterol content from changes in fluidity in living cell membranes. Biophys J. 2013; 104:1238–1247. [PubMed: 23528083]

Goudriaan JR, Dahlmans VE, Febbraio M, Teusink B, Romijn JA, Havekes LM, Voshol PJ. Intestinal lipid absorption is not affected in CD36 deficient mice. Mol Cell Biochem. 2002; 239:199–202. [PubMed: 12479586]

Harmon CM, Luce P, Abumrad NA. Labelling of an 88 kDa adipocyte membrane protein by sulpho-N-succinimidyl long-chain fatty acids: inhibition of fatty acid transport. Biochem Soc Trans. 1992; 20:811–813. [PubMed: 1487069]

Hashidate-Yoshida T, Harayama T, Hishikawa D, Morimoto R, Hamano F, Tokuoka SM, Eto M, Tamura-Nakano M, Yanobu-Takanashi R, Mukumoto Y, et al. Fatty acid remodeling by LPCAT3 enriches arachidonate in phospholipid membranes and regulates triglyceride transport. Elife. 2015; 4

Hjelte L, Melin T, Nilsson A, Strandvik B. Absorption and metabolism of [3H]arachidonic and [14C]linoleic acid in essential fatty acid-deficient rats. Am J Physiol. 1990; 259:G116–124. [PubMed: 2115302]

Ho SY, Storch J. Common mechanisms of monoacylglycerol and fatty acid uptake by human intestinal Caco-2 cells. Am J Physiol Cell Physiol. 2001; 281:C1106–1117. [PubMed: 11546646]

Kamp F, Hamilton JA. pH gradients across phospholipid membranes caused by fast flip-flop of un-ionized fatty acids. Proc Natl Acad Sci U S A. 1992; 89:11367–11370. [PubMed: 1454821]

Levy E, Garofalo C, Thibault L, Dionne S, Daoust L, Lepage G, Roy CC. Intraluminal and intracellular phases of fat absorption are impaired in essential fatty acid deficiency. Am J Physiol. 1992; 262:G319–326. [PubMed: 1539663]

Ling KY, Lee HY, Hollander D. Mechanisms of linoleic acid uptake by rabbit small intestinal brush border membrane vesicles. Lipids. 1989; 24:51–55. [PubMed: 2747430]

Murota K, Storch J. Uptake of micellar long-chain fatty acid and sn-2-monoacylglycerol into human intestinal Caco-2 cells exhibits characteristics of protein-mediated transport. J Nutr. 2005; 135:1626–1630. [PubMed: 15987840]

Nassir F, Wilson B, Han X, Gross RW, Abumrad NA. CD36 is important for fatty acid and cholesterol uptake by the proximal but not distal intestine. J Biol Chem. 2007; 282:19493–19501. [PubMed: 17507371]

Nauli AM, Nassir F, Zheng S, Yang Q, Lo CM, Vonlehmden SB, Lee D, Jandacek RJ, Abumrad NA, Tso P. CD36 is important for chylomicron formation and secretion and may mediate cholesterol uptake in the proximal intestine. Gastroenterology. 2006; 131:1197–1207. [PubMed: 17030189]

Parasassi T, Gratton E. Membrane lipid domains and dynamics as detected by Laurdan fluorescence. J Fluoresc. 1995; 5:59–69. [PubMed: 24226612]

Provensi G, Coccurello R, Umehara H, Munari L, Giacovazzo G, Galeotti N, Nosi D, Gaetani S, Romano A, Moles A, et al. Satiety factor oleoylethanolamide recruits the brain histaminergic system to inhibit food intake. Proc Natl Acad Sci U S A. 2014; 111:11527–11532. [PubMed: 25049422]

Barnes, Richard H.; Miller, Elmer S.; Burr, a.G.O. FAT ABSORPTION IN ESSENTIAL FATTY ACID DEFICIENCY. J. Biol. Chem. 1941; 140:773–778.

Rodriguez de Fonseca F, Navarro M, Gomez R, Escuredo L, Nava F, Fu J, Murillo-Rodriguez E, Giuffrida A, LoVerme J, Gaetani S, et al. An anorexic lipid mediator regulated by feeding. Nature. 2001; 414:209–212. [PubMed: 11700558]

Rong X, Albert CJ, Hong C, Duerr MA, Chamberlain BT, Tarling EJ, Ito A, Gao J, Wang B, Edwards PA, et al. LXRs regulate ER stress and inflammation through dynamic modulation of membrane phospholipid composition. Cell Metab. 2013; 18:685–697. [PubMed: 24206663]

Rong X, Wang B, Dunham MM, Hedde PN, Wong JS, Gratton E, Young SG, Ford DA, Tontonoz P. Lpcat3-dependent production of arachidonoyl phospholipids is a key determinant of triglyceride secretion. Elife. 2015; 4

Schwartz GJ, Fu J, Astarita G, Li X, Gaetani S, Campolongo P, Cuomo V, Piomelli D. The lipid messenger OEA links dietary fat intake to satiety. Cell Metab. 2008; 8:281–288. [PubMed: 18840358]

Shim J, Moulson CL, Newberry EP, Lin MH, Xie Y, Kennedy SM, Miner JH, Davidson NO. Fatty acid transport protein 4 is dispensable for intestinal lipid absorption in mice. J Lipid Res. 2009; 50:491–500. [PubMed: 18843142]

Skala I, Konradova V. Hypertrophy of the small intestine after its partial resection in the rat. Ultrastructure of the intestinal epithelium. Am J Dig Dis. 1969; 14:182–188. [PubMed: 5773914]

Soria-Gomez E, Bellocchio L, Reguero L, Lepousez G, Martin C, Bendahmane M, Ruehle S, Remmers F, Desprez T, Matias I, et al. The endocannabinoid system controls food intake via olfactory processes. Nat Neurosci. 2014; 17:407–415. [PubMed: 24509429]

Spector AA, Yorek MA. Membrane lipid composition and cellular function. J Lipid Res. 1985; 26:1015–1035. [PubMed: 3906008]

Stahl A, Hirsch DJ, Gimeno RE, Punreddy S, Ge P, Watson N, Patel S, Kotler M, Raimondi A, Tartaglia LA, et al. Identification of the major intestinal fatty acid transport protein. Mol Cell. 1999; 4:299–308. [PubMed: 10518211]

Temel RE, Lee RG, Kelley KL, Davis MA, Shah R, Sawyer JK, Wilson MD, Rudel LL. Intestinal cholesterol absorption is substantially reduced in mice deficient in both ABCA1 and ACAT2. J Lipid Res. 2005; 46:2423–2431. [PubMed: 16150828]

Trotter PJ, Ho SY, Storch J. Fatty acid uptake by Caco-2 human intestinal cells. J Lipid Res. 1996; 37:336–346. [PubMed: 9026531]

Tso P, Balint JA, Simmonds WJ. Role of biliary lecithin in lymphatic transport of fat. Gastroenterology. 1977; 73:1362–1367. [PubMed: 410697]

Tso P, Kendrick H, Balint JA, Simmonds WJ. Role of biliary phosphatidylcholine in the absorption and transport of dietary triolein in the rat. Gastroenterology. 1981; 80:60–65. [PubMed: 6893826]

Tso P, Lam J, Simmonds WJ. The importance of the lysophosphatidylcholine and choline moiety of bile phosphatidylcholine in lymphatic transport of fat. Biochim Biophys Acta. 1978; 528:364–372. [PubMed: 638162]

Tso P, Nauli A, Lo CM. Enterocyte fatty acid uptake and intestinal fatty acid-binding protein. Biochem Soc Trans. 2004; 32:75–78. [PubMed: 14748716]

Werner A, Minich DM, Havinga R, Bloks V, Van Goor H, Kuipers F, Verkade HJ. Fat malabsorption in essential fatty acid-deficient mice is not due to impaired bile formation. Am J Physiol Gastrointest Liver Physiol. 2002; 283:G900–908. [PubMed: 12223350]

Xie Y, Newberry EP, Young SG, Robine S, Hamilton RL, Wong JS, Luo J, Kennedy S, Davidson NO. Compensatory increase in hepatic lipogenesis in mice with conditional intestine-specific Mttp deficiency. J Biol Chem. 2006; 281:4075–4086. [PubMed: 16354657]

Yen CL, Cheong ML, Grueter C, Zhou P, Moriwaki J, Wong JS, Hubbard B, Marmor S, Farese RV Jr. Deficiency of the intestinal enzyme acyl CoA:monoacylglycerol acyltransferase-2 protects mice from metabolic disorders induced by high-fat feeding. Nat Med. 2009; 15:442–446. [PubMed: 19287392]

Yurkowski M, Walker BL. The molecular species of mucosal phosphatidyl cholines from the small intestine of normal and essential fatty acid-deficient rats. Biochim Biophys Acta. 1971; 231:145–152. [PubMed: 5546573]

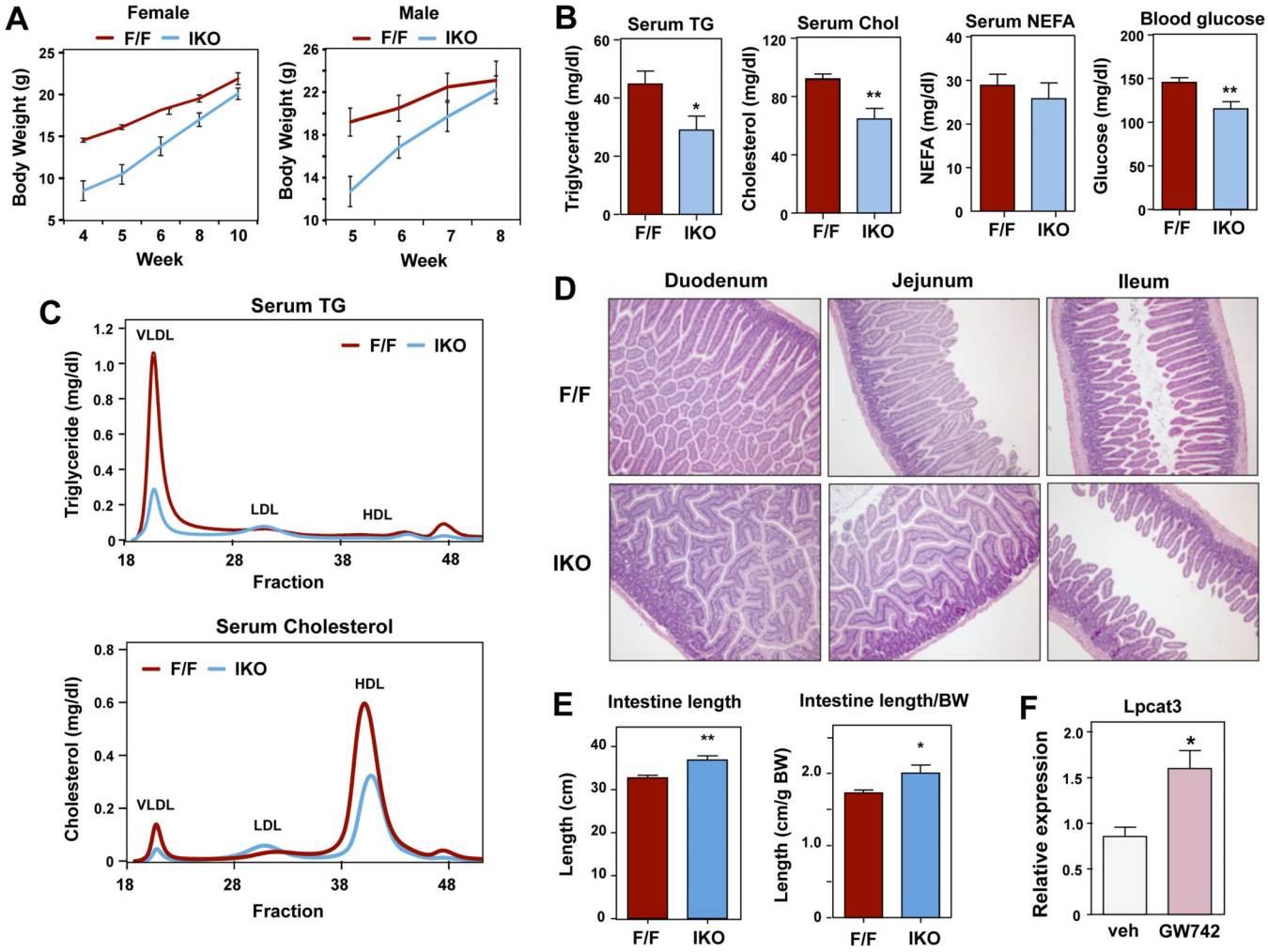

Figure 1. Reduced plasma triglyceride and cholesterol levels in intestine-specific Lpcat3 knockout mice

(**A**) Growth curve of *Lpcat3*$^{fl/fl}$ (F/F) and *Lpcat3*$^{fl/fl}$ *Villin-Cre* (IKO) mice on chow diet after weaning (n≥6/group).

(**B**) Plasma lipid and glucose levels in 8-10 week old chow-diet fed *Lpcat3*$^{fl/fl}$ (F/F) and *Lpcat3*$^{fl/fl}$ *Villin-Cre* (IKO) mice (n≥6/group). Mice were fasted for 6 h before blood collection.

(**C**) Lipoprotein profiles of *Lpcat3*$^{fl/fl}$ (F/F) and *Lpcat3*$^{fl/fl}$ *Villin-Cre* (IKO) mice. Plasma from F/F and IKO mice was pooled (n=5) and analyzed by fast protein liquid chromatography (FPLC).

(**D**) Hematoxylin and eosin (H&E) staining of intestine sections from *Lpcat3*$^{fl/fl}$ (F/F) and *Lpcat3*$^{fl/fl}$ *Villin-Cre* (IKO) mice.

(**E**) Small intestine length of *Lpcat3*$^{fl/fl}$ (F/F) and *Lpcat3*$^{fl/fl}$ *Villin-Cre* (IKO) mice (n≥6/group).

(**F**) Induction of Lpcat3 mRNA expression in intestines of mice treated with 20 mg/kg/day GW742 by oral gavage for 5 days (n=5/group). Gene expression was measured by real-time PCR.

Values are means ± SEM. Statistical analysis was performed with Student's t test. *$p < 0.05$; **$p < 0.01$.

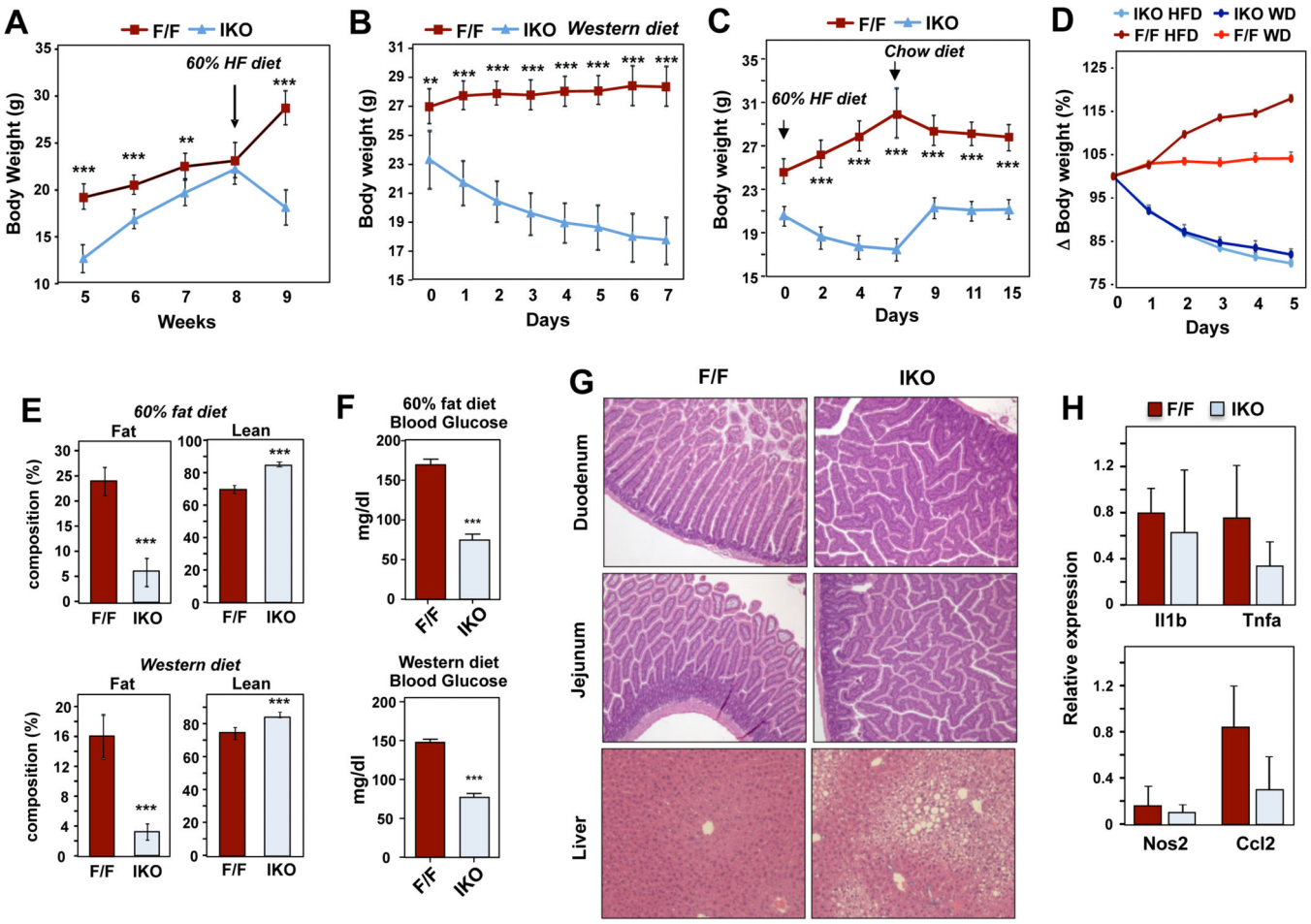

Figure 2. Mice lacking Lpcat3 cannot survive on high-fat diet or Western diet

(**A-B**) Growth curve of male *Lpcat3*$^{fl/fl}$ (F/F) and *Lpcat3*$^{fl/fl}$ *Villin-Cre* (IKO) mice placed on chow diet after weaning and then switched to 60% high-fat diet (HFD) (A) (n≥6/group), or Western diet (B) (n≥4/group).

(**C**) Growth curve of female *Lpcat3*$^{fl/fl}$ (F/F) and *Lpcat3*$^{fl/fl}$ *Villin-Cre* (IKO) mice on 60% HFD for 7 days and switched back to chow diet (n≥4/group).

(**D**) Body weight change in 60% HFD and western diet fed mice (n≥4/group).

(**E**) Body composition of *Lpcat3*$^{fl/fl}$ (F/F) and *Lpcat3*$^{fl/fl}$ *Villin-Cre* (IKO) mice on 60% HFD for 10 days (n≥6/group) and Western diet for 8 days (n≥4/group).

(**F**) Blood glucose levels in *Lpcat3*$^{fl/fl}$ (F/F) and *Lpcat3*$^{fl/fl}$ *Villin-Cre* (IKO) mice on 60% HFD and Western Diet as in (D).

(**G**) H&E staining of intestine and liver sections from *Lpcat3*$^{fl/fl}$ (F/F) and *Lpcat3*$^{fl/fl}$ *Villin-Cre* (IKO) mice on 60% HFD for 10 days.

(**H**) Expression of inflammatory genes in fasting and 60% HFD refed intestines measured by real-time PCR (n≥4/group).

Values are means ± SEM. Statistical analysis was performed with two-way ANOVA (A-D) and Student's t test (E, F and H). *p < 0.05, **p < 0.01, *** p<0.001.

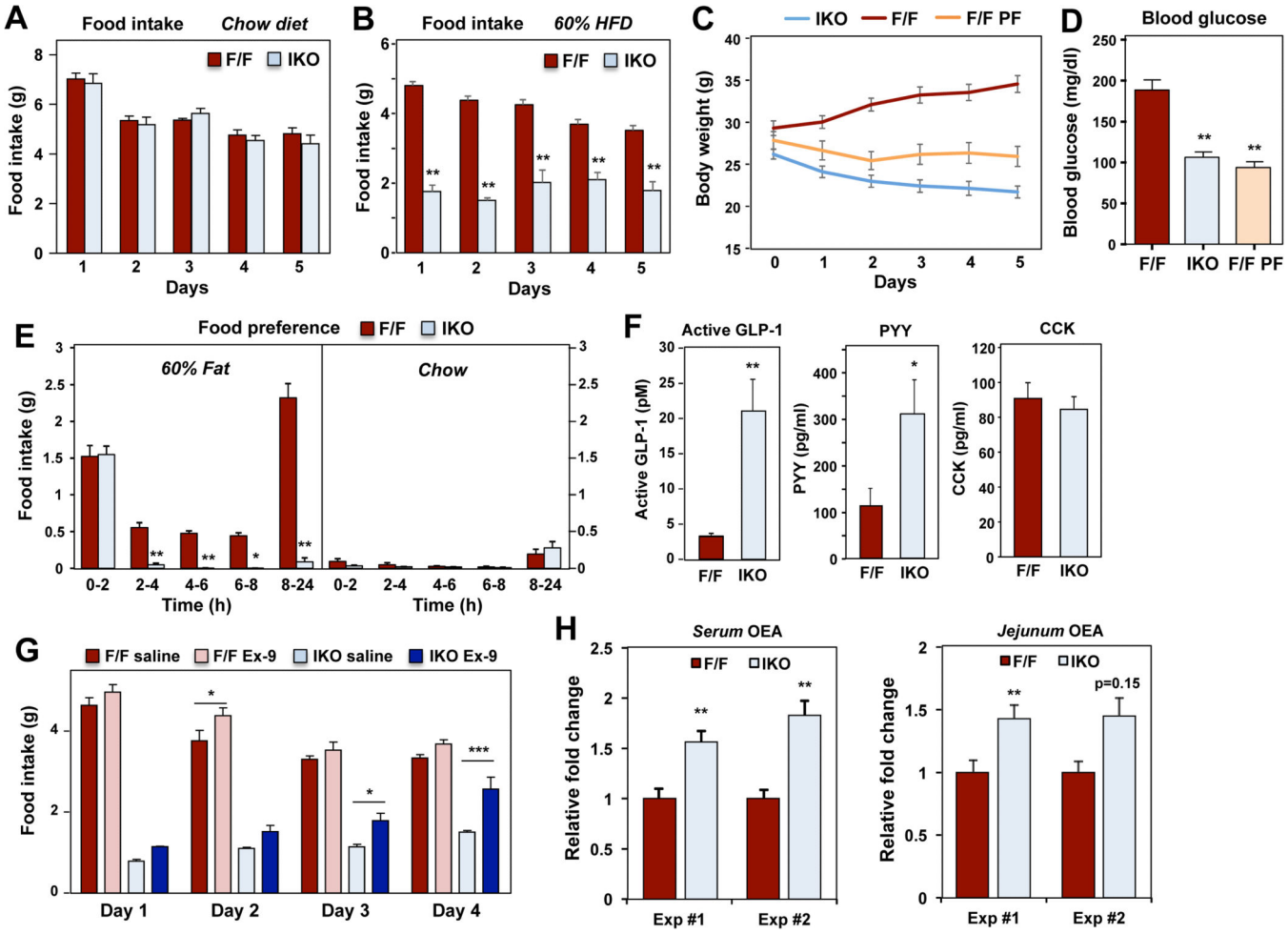

Figure 3. Triglyceride-rich diets inhibit feeding in Lpcat3 IKO mice

(**A-B**) Daily food intake in male *Lpcat3*$^{fl/fl}$ (F/F) and *Lpcat3*$^{fl/fl}$ *Villin-Cre* (IKO) mice on chow diet (A) and 60% HFD (B).

(**C**) Growth curve of male *Lpcat3*$^{fl/fl}$ (F/F), *Lpcat3*$^{fl/fl}$ *Villin-Cre* (IKO) and pair feeding *Lpcat3*$^{fl/fl}$ (F/F PF) mice (n≥5/group).

(**D**) Blood glucose levels in mice as in (D).

(**E**) Food preference test in female *Lpcat3*$^{fl/fl}$ (F/F), *Lpcat3*$^{fl/fl}$ *Villin-Cre* (IKO) during fasting/refeeding. Mice were fasted overnight and provided with both 60% HFD and chow diet. Food intake was monitored for 24 h (n≥5/group).

(**F**) ELISA analysis of active GLP-1, PYY and CCK in the plasma of *Lpcat3*$^{fl/fl}$ (F/F) and *Lpcat3*$^{fl/fl}$ *Villin-Cre* (IKO) mice fasted overnight and refed 60% HFD for 2 h (n≥5/group).

(**G**) Food intake in *Lpcat3*$^{fl/fl}$ (F/F) and *Lpcat3*$^{fl/fl}$ *Villin-Cre* (IKO) mice treated with vehicle or GLP-1 receptor antagonist Ex-9 (n=3/group). Mice were fed 60% HFD and i.p. injected with Ex-9 (5 μg/25 g BW, twice/day) for 5 days.

(**H**) Mass spectrometry analysis of OEA in the serum and jejunum of mice fasted overnight and refed 60% HFD (n≥4/group). Results from two independent experiments are shown.

Values are means ± SEM. Statistical analysis was performed with two-way ANOVA (AC, E and G-J), one-way ANOVA (D), and Student's t test (F, and H). *$p < 0.05$; **$p < 0.01$, *** $p<0.001$, ns, not significant.

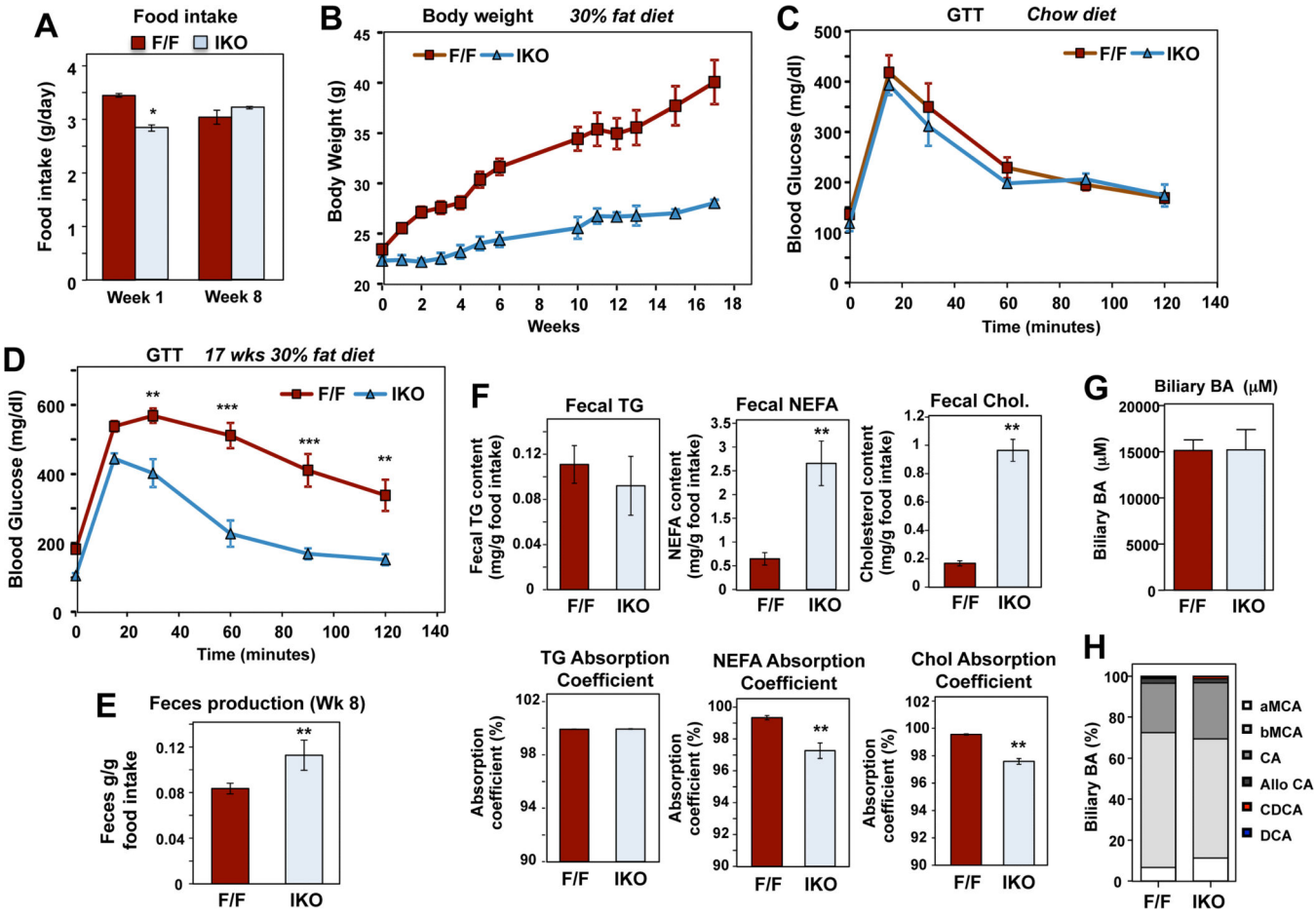

Figure 4. Lpcat3 IKO mice are protected from diet-induced obesity

(**A**) Average food intake in male *Lpcat3*$^{fl/fl}$ (F/F) and *Lpcat3*$^{fl/fl}$ *Villin-Cre* (IKO) mice after week 1 and week 8 of 30% fat diet feeding (n≥5/group).

(**B**) Growth curve of *Lpcat3*$^{fl/fl}$ (F/F) and *Lpcat3*$^{fl/fl}$ *Villin-Cre* (IKO) mice on 30% fat diet.

(**C-D**) Glucose tolerance tests (GTT) performed *Lpcat3*$^{fl/fl}$ (F/F) and *Lpcat3*$^{fl/fl}$ *Villin-Cre* (IKO) mice before 30% fat feeding (chow diet) (C) and after feeding 30% fat diet for 17 weeks (D).

(**E**) Fecal production in *Lpcat3*$^{fl/fl}$ (F/F) and *Lpcat3*$^{fl/fl}$ *Villin-Cre* (IKO) mice during week 8 of 30% fat diet feeding.

(**F**) Fecal lipid levels and lipid absorption coefficient in *Lpcat3*$^{fl/fl}$ (F/F) and *Lpcat3*$^{fl/fl}$ *Villin-Cre* (IKO) mice during week 8 of 30% fat diet feeding.

(**G-H**) Total biliary bile acid (BA) levels and species composition in chow diet fed *Lpcat3*$^{fl/fl}$ (F/F) and *Lpcat3*$^{fl/fl}$ *Villin-Cre* (IKO) (n≥6/group).

Values are means ± SEM. Statistical analysis was performed with Student's t test (A, E and F), and two-way ANOVA (C-D). *p < 0.05; **p < 0.01.

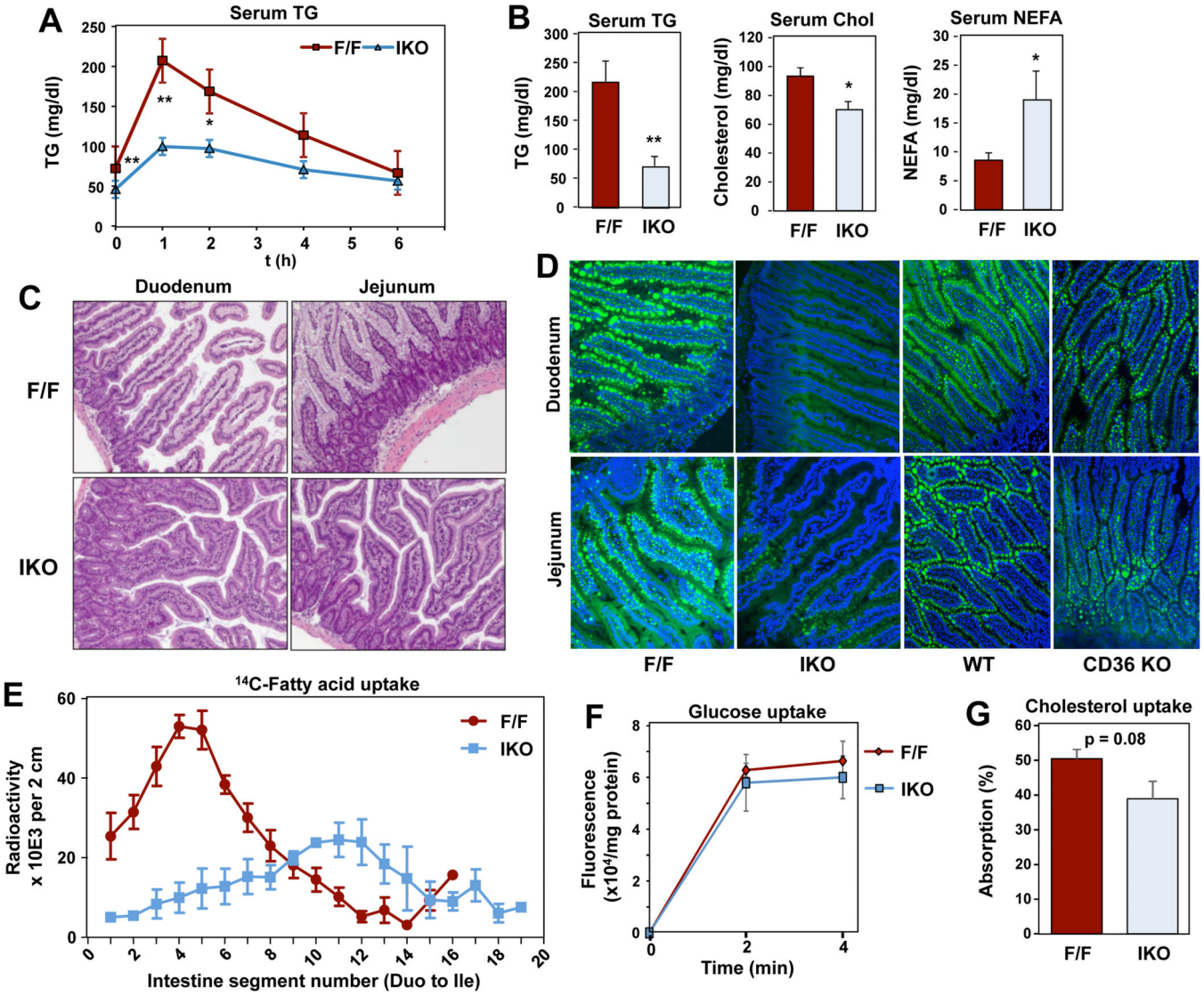

Figure 5. Impaired triglyceride absorption in Lpcat3 IKO mice

(**A**) Postprandial TG response in male *Lpcat3*$^{fl/fl}$ (F/F) and *Lpcat3*$^{fl/fl}$ *Villin-Cre* (IKO) mice after oral gavage with olive oil (10 μl/g BW) (n=6/group).

(**B**) Plasma lipid levels in chow diet fed male *Lpcat3*$^{fl/fl}$ (F/F) and *Lpcat3*$^{fl/fl}$ *Villin-Cre* (IKO) mice after fasting overnight and refeeding 60% HFD for 2 h. (n≥4/group)

(**C**) H&E staining of intestine sections from *Lpcat3*$^{fl/fl}$ (F/F) and *Lpcat3*$^{fl/fl}$ *Villin-Cre* (IKO) mice as in (C).

(**D**) Fluorescence images of small intestines of *Lpcat3*$^{fl/fl}$ (F/F) and *Lpcat3*$^{fl/fl}$ *Villin-Cre* (IKO) mice, and wild-type C57BL/6 and *Cd36*−/− mice after oral gavage with olive oil containing BODIPY-labeled fatty acid for 2 h.

(**E**) Distribution of radioactivity in intestinal segments of male *Lpcat3*$^{fl/fl}$ (F/F) and *Lpcat3*$^{fl/fl}$ *Villin-Cre* (IKO) mice after an oral challenge of olive oil containing ^{14}C-trioleoylglycerol for 2 h (n=3/group).

(**F**) *Ex vivo* glucose uptake assay in *Lpcat3*$^{fl/fl}$ (F/F) and *Lpcat3*$^{fl/fl}$ *Villin-Cre* (IKO) intestines (n=3/group).

(**G**) *In vivo* cholesterol absorption measured by fecal dual isotope ratio method (n=4/group). Values are means ± SEM. Statistical analysis was performed with two-way ANOVA (A and G) and Student's t test (B and F). *$p < 0.05$; **$p < 0.01$.

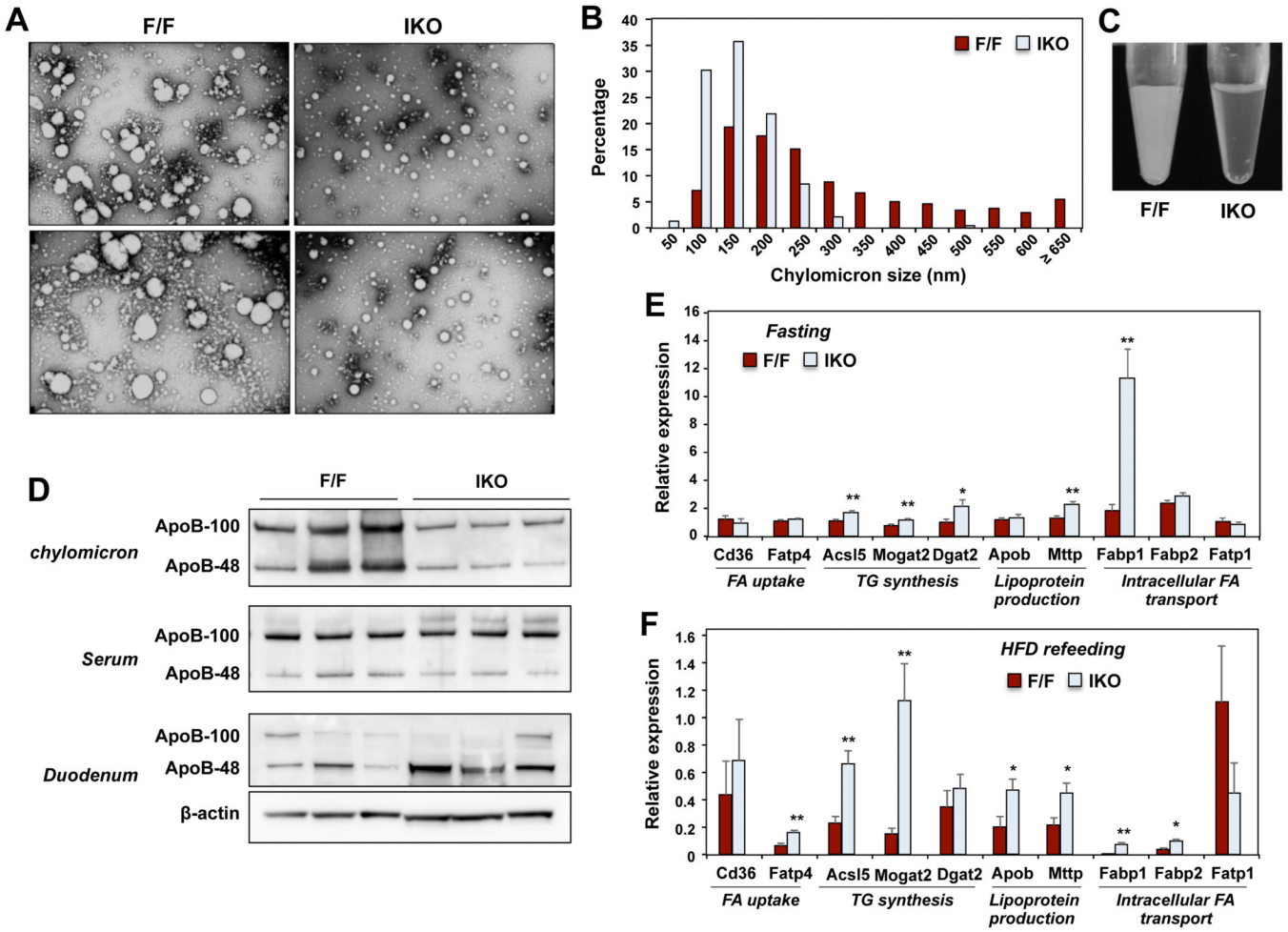

Figure 6. Loss of Lpcat3 in intestine impairs chylomicron lipidation and secretion

(**A**) Plasma chylomicron particle size in *Lpcat3*$^{fl/fl}$ (F/F) and *Lpcat3*$^{fl/fl}$ *Villin-Cre* (IKO) mice. Mice were fasted overnight and refed 60% HFD for 2 h. Chylomicrons were isolated and pooled from 5 mice/group. Chylomicrons were stained with 2.0% uranyl acetate and visualized by electron microscopy.

(**B**) Quantification of chylomicron particle size in (A).

(**C**) Representative pictures of plasma collected from *Lpcat3*$^{fl/fl}$ (F/F) and *Lpcat3*$^{fl/fl}$ *Villin-Cre* (IKO) mice as in (A).

(**D**) ApoB western blot in chylomicron, whole serum and duodenum of *Lpcat3*$^{fl/fl}$ (F/F) and *Lpcat3*$^{fl/fl}$ *Villin-Cre* (IKO) mice as in (A).

(**E-F**) Gene expression in jejunum of *Lpcat3*$^{fl/fl}$ (F/F) and *Lpcat3*$^{fl/fl}$ *Villin-Cre* (IKO) mice during fasting (E) and 60% HFD refeeding (F) mice (n≥4/group).

Values are means ± SEM. Statistical analysis was performed with Student's t test. *p < 0.05; **p < 0.01.

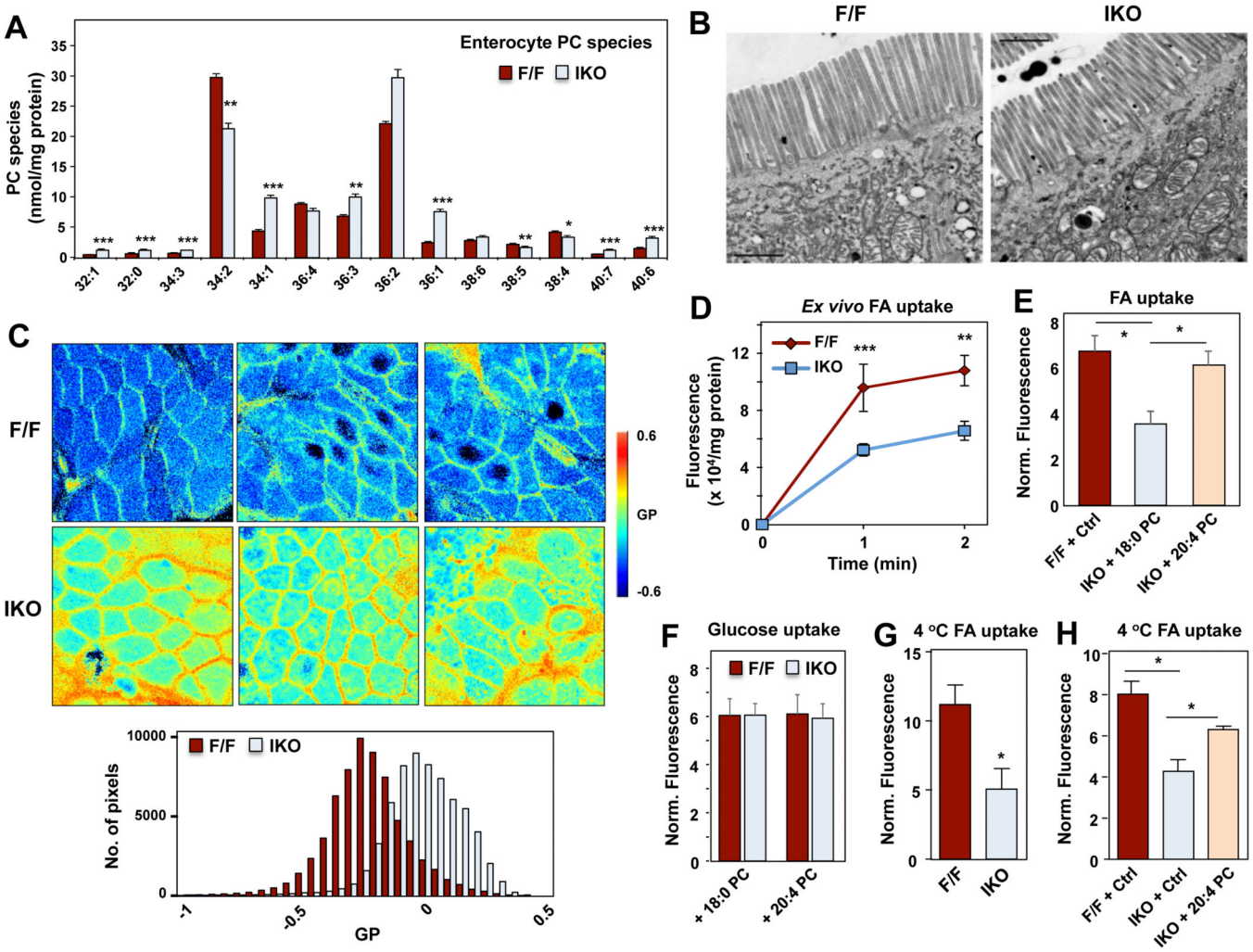

Figure 7. Lpcat3 deficiency impairs linoleate incorporation and reduces enterocyte membrane dynamics

(**A**) ESI-MS/MS analysis of the abundance of PC species in enterocytes from male *Lpcat3*$^{fl/fl}$ (F/F) and *Lpcat3*$^{fl/fl}$ *Villin-Cre* (IKO) mice fed 60% HFD for 5 days (n ≥ 5/group).

(**B**) Electron microscopy analysis of microvilli of enterocytes from *Lpcat3*$^{fl/fl}$ (F/F) and *Lpcat3*$^{fl/fl}$ *Villin-Cre* (IKO) mice.

(**C**) Laurdan imaging of enterocyte membrane dynamics. Duodenum from male *Lpcat3*$^{fl/fl}$ (F/F) and *Lpcat3*$^{fl/fl}$ *Villin-Cre* (IKO) mice were stained with laurdan. The laurdan emission spectrum was captured by a 2-photon laser-scan microscope. Generalized polarization (GP) was calculated from the emission intensities obtained from images.

Higher GP value indicates that membranes are more ordered and less dynamic. The GP value of each pixel was used to generate a pseudocolor GP image. The binary histograms of the GP distribution of the GP images were quantified at the bottom (n = 4).

(**D**) *Ex vivo* fatty acid uptake in duodenum of male *Lpcat3*$^{fl/fl}$ (F/F) and *Lpcat3*$^{fl/fl}$ *Villin-Cre* (IKO) mice at room temperature. Mice were fasted for 4 h followed by fatty acid uptake assay as described in the methods (n=5/group).

(**E**) *Ex vivo* fatty acid uptake in duodenum treated with 16:0; 18:0 PC (control) and 16:0, 20:4 PC at room temperature (n=4/group).
(**F**) *Ex vivo* glucose uptake in duodenum of male *Lpcat3*$^{fl/fl}$ (F/F) and *Lpcat3*$^{fl/fl}$ *Villin-Cre* (IKO) mice treated with 16:0; 18:0 PC (control) and 16:0, 20:4 PC (n=4/group) at room temperature (n=5/group).
(**G**) *Ex vivo* fatty acid uptake in duodenum of female *Lpcat3*$^{fl/fl}$ (F/F) and *Lpcat3*$^{fl/fl}$ *Villin-Cre* (IKO) mice at 0°C on ice (n=3/group).
(**H**) *Ex vivo* fatty acid uptake in duodenum treated with 16:0; 18:0 PC (control) and 16:0, 20:4 PC at 4°C on ice (n=3/group).
Values are means ± SEM. Statistical analysis was performed with Student's t test (A and G), one-way ANOVA (E and H) and two-way ANOVA (D and F). *$p < 0.05$; **$p < 0.01$; ***$p<0.001$.